1. Title page

Tissue Identification in a Porcine Model by Differential Ion Mobility Spectrometry Analysis of Surgical Smoke

Anton Kontunen[1], Markus Karjalainen[1], Jukka Lekkala[1], Antti Roine*[2], Niku Oksala*[3,4,5]

*Authors contributed equally

[1]BioMediTech Institute and Faculty of Biomedical Sciences and Engineering, Tampere University of Technology, PL 527, 33720 Tampere, Finland, anton.kontunen@tut.fi

[2]Department of Surgery, Hatanpää Hospital, Tampere, Hatanpäänkatu 24, 33900 Tampere

[3]Division of Vascular Surgery, Tampere University Hospital; [4]Faculty of Medicine and Life Sciences, University of Tampere, Finland; [5]Finnish Cardiovascular Research Center, Tampere, Finland

Abbreviated title for the running head: Tissue identification from surgical smoke by DMS

Corresponding author: Anton Kontunen

Address: Korkeakoulunkatu 10, 33720 Tampere

Phone: 040 198 1160

Email: anton.kontunen@tut.fi

2. Abstract and key terms

Electrosurgery is widely used in various surgical operations. When tissue is cut with high-frequency current, the cell contents at the incision area evaporate and together with water and possible soot particles, form surgical smoke. The smoke contains cell metabolites, and therefore, possible biomarkers for cancer or bacterial infection. Thus, the analysis of surgical smoke could be used in intraoperative medical diagnostics. We present a method that can be used to detect the characteristics of various tissue types by means of differential ion mobility spectrometry (DMS) analysis of surgical smoke. We used our method to test tissue identification with ten different porcine tissues. We classified the DMS responses with cross-validated linear discriminant analysis models. The classification accuracy in a measurement set with ten tissue types was 95%. The presented tissue identification by DMS analysis of surgical smoke is a proof-of-concept, which opens the possibility to research the method in diagnosing human tissues and diseases in the future.

Key terms: FAIMS, electrosurgery, LDA, VOC

Abbreviations: differential ion mobility spectrometry (DMS), high-field asymmetric waveform ion mobility spectrometry (FAIMS), linear discriminant analysis (LDA), rapid evaporative ionization mass spectrometry (REIMS), mass spectrometry (MS), leave-one-out cross-validation (LOOCV), automatic tissue analysis system (ATAS), voltage amplitude of the asymmetric waveform (V_{RF}), voltage of the DC compensation field (V_C), volatile organic compound (VOC)

3. Introduction

Electrosurgery, also known as *diathermy*, is one of the most common energy-based surgical methods[2]. In electrosurgery, high-frequency (200 kHz – 3.3 MHz) alternating current (AC) is conducted to the patient by either a monopolar or bipolar electrode[10]. Depending on the properties of the AC signal, the electrosurgical instrument can either *cut* (high voltage, continuous waveform) or *coagulate* (low voltage, pulsed waveform) the tissue. Especially in the cut mode, the surgical electrode vaporizes the cell contents and produces *surgical smoke*.

Surgical smoke primarily consists of water, but the organic matter of the cells is also simultaneously evaporated[20]. This means that surgical smoke carries information about the excised tissue in the form of possible biomarkers or tissue-specific metabolites. Metabolites can be used to differentiate the type and state of tissues, as proven by Schäfer et al., who introduced a method for analyzing the surgical smoke created in electrosurgery in 2009[16]. Since then, the method has been extensively studied for numerous medical and food industry applications[3,4,18,21]. For example, in the most recent publication regarding ex vivo breast cancer identification from benign breast tissue, the method achieved 93.4% sensitivity and 94.9% specificity[18]. Although the results have been excellent in terms of diagnostic properties, the method has still not spread to clinical use. One reason for this is perhaps that the *Rapid Evaporative Ionization Mass Spectrometry* (REIMS) relies on the use of an expensive mass spectrometer (MS), which together with the *Intelligent Knife* (also known as *iKnife*) sampling system used in the studies can cost several hundred thousand dollars. Other potential factors hindering the clinical use are regulatory approvals and lack of evidence in large cohorts of heterogeneous tissues. In addition, the miniaturization of high-performance MS is challenging, making its use in an operating room problematic due to space constraints.

Despite its limitations, a system like the REIMS, which could accurately detect the excised tissue type during surgery, would be in high demand in the healthcare market. For example, in breast cancer surgeries, reoperations due to residual tumor tissue caused by errors in cancer margin detection are common and add to the total healthcare costs significantly[13]. The current gold standard for intraoperative cancer margin evaluation is histopathological examination from a frozen section. The examination is expensive, and it disrupts the flow of the operation, since the operating staff and anesthetized patient are forced to wait for the results for tens of minutes.

Besides the REIMS system, other methods that aim to help in intraoperative cancer margin detection have been introduced. One example of a commercially available device is the MarginProbe (Dune Medical Devices Ltd, Caesarea, Israel), which uses *Radio-Frequency Spectroscopy* to assess the differences in breast tissue[1]. In a recent study, the use of the MarginProbe lowered the number of reoperations by 61%[9]. However, using an additional tool during surgery means that the flow of the operation is disturbed.

To create a system that does not affect the workflow of the surgeon, we propose tissue analysis by *Ion Mobility Spectrometry* (IMS). IMS is a method similar to MS, but the main difference is that while MS requires a vacuum to operate, IMS operates in atmospheric pressure. This means that in IMS, the molecules of the medium collide

with the measured target ions[7]. Additionally, in contrast to MS, which separates molecules according to their mass and charge, IMS separates molecules based on their ion mobility, which is a combination of the electrical charge and the shape of a molecule. Furthermore, IMS devices are not only considerably cheaper and more compact than MS devices, they are also easier to produce and maintain. The main downside of IMS compared to MS is its inferior resolving power, which is due to the fact that it operates in atmospheric pressure. The resolving power can be considered as the capability of the device to differentiate overlapping ion peaks in the output spectrum.

To increase the resolving power, IMS technology has been developed further with the introduction of *Differential Ion Mobility Spectrometry* (DMS), also known as *High-field Asymmetric Waveform Ion Mobility Spectrometry* (FAIMS)[7]. In DMS, the use of a radio-frequency (RF) waveform orthogonal to the sample flow is used to further separate the sample molecules. This increases the resolving power beyond the capabilities of traditional IMS, but it is still significantly lower than in MS devices[7,22]. Despite its inferior resolving power, DMS is a tempting alternative to the cumbersome MS due to its simplicity, lower cost, and size. To our knowledge, there are no publications about the use of IMS or DMS methods to analyze surgical smoke.

In this study, we introduce a DMS-based tissue analysis system and evaluate its applicability in the discrimination of porcine tissues based on smoke created in electrosurgery. Since the availability and ethical considerations limit the use of human tissues, we considered porcine tissue as the most suitable alternative sample material for this proof-of-concept study.

4. Materials and Methods

Study Material

We obtained the tissues of a Finnish landrace pig (Sus scrofa domesticus) from a slaughterhouse (Paijan Tilateurastamo, Urjala, Finland). The tissues were slaughterhouse offal including tongue, lungs, kidneys, heart, liver, skeletal muscle, skin with subcutaneous fat, and brains. After transportation in a thermally insulated container, we stored the fresh tissue samples in a freezer at -18 °C. We froze the tissues to prevent tissue degradation during the research. We conducted the measurement phases in four weeks. Before each measurement set, we individually thawed the tissue samples and placed them on the measurement platform for analysis at room temperature. In long measurement sets (>30 min), the sample pieces were moisturized with de-ionized water using a spray bottle. The tissue samples were all from the same single animal except for the brains, since they were too small to accommodate all 60 cuts. In total 14 porcine brains were required for the measurements of gray and white matter.

Measurement Protocol

We conducted the tissue identification measurements in three phases:

Phase I: We selected five histologically distinct tissue types (skeletal muscle, fat, renal cortex, liver and lung). We performed ten electrosurgical cuts to each tissue in non-randomized order, resulting in fifty measurements. We also conducted ten ‘’empty’’ cuts, in which we turned on the knife without it touching any tissue and measured the DMS response. We added the empty cuts to the first measurement set to ensure that each tissue produced a measurable output response that could be distinguished from the baseline response. The total number of cuts in the pilot phase was chosen so that it would be possible to conduct the pilot phase in one working day. A schematic of the cutting protocol can be seen in Figure 1.

Phase II: We extended the series to ten anatomically distinct tissue types (gray and white matter of the brain, liver, skeletal muscle, subcutaneous fat, lung, renal cortex, skin, tongue and cardiac muscle). We conducted sixty cuts per tissue for a total of 600 measurements. A picture of a piece of skeletal muscle after the phase II measurements can be seen in Figure 2.

Phase III: We used the remaining tissue material from phase II to further validate the results from the previous phases by analyzing a set of four tissues (renal cortex, fat, skeletal muscle and liver). We conducted this additional small set in order to account for the possible inter-day variability of measurement conditions in the second phase. We conducted ten cuts per tissue in a randomized order for a total of forty measurements. The number of cuts was limited by the amount of available sample material left after phase II.

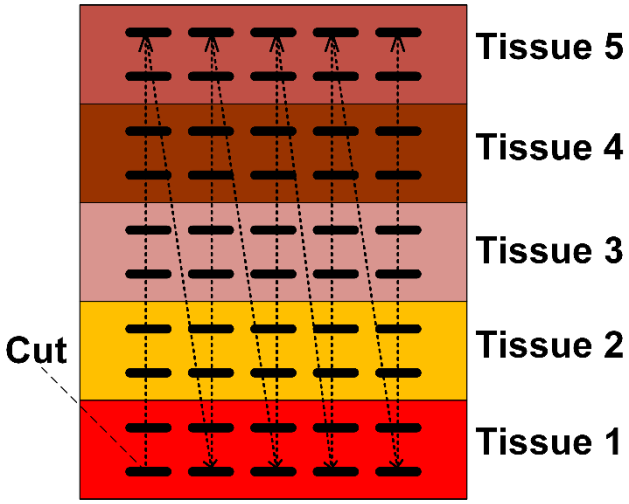

Figure 1. The order of the cuts in phase I. The empty cuts were made consecutively after the tissue cuts.

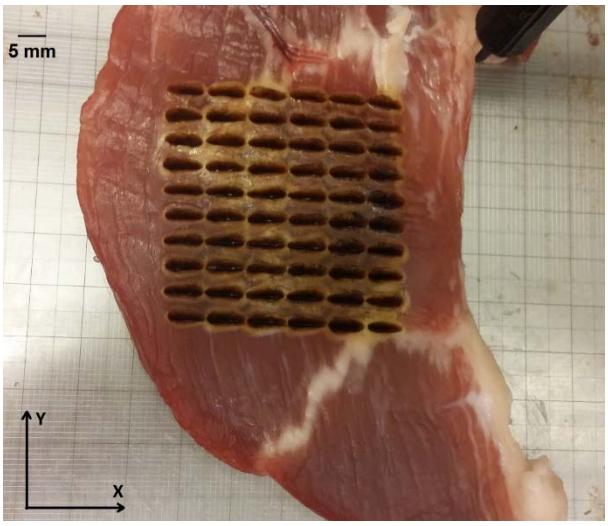

Figure 2. A piece of skeletal muscle after the measurement sequence of 60 cuts in phase II. The order of the cuts followed a similar pattern as shown in Figure 1.

The Measurement System

The measurement system we developed in this study can be divided into three distinct functional modules: automated electrosurgical sampling, sample modification (filtration and dilution), and sample detection by the ENVI-AMC® DMS device (Environics Oy, Finland). Due to the combination of the (semi-)automatic sampling system and its end-purpose, we have called our system the *automatic tissue analysis system* (ATAS).

The surgical device in the electrosurgical sampling stage of the ATAS was a medical grade system *Itkacut 350MB* (Innokas Medical Oy, Finland). The device worked with constant voltage without impedance compensation, which influenced the choice for the nominal cutting power. We selected the cutting power for the measurements with the aim of producing enough surgical smoke regardless of the tissue impedance. In the preliminary testing, it seemed that the subcutaneous fat in particular did not produce measurable concentrations of smoke with the traditionally used low cutting powers (~40 W). In order to obtain surgical smoke from all tissues, we chose 120 W

as the nominal cutting power of the surgical electrode. The electrode was a standard *monopolar knife electrode* (HF 9805-24, HEBUmedical GmbH, Germany).

The electrode was controlled by a customized *computerized numerical control* (CNC) device (REPRAP Mendel Prusa i3 kit, KitPrinter3D, Spain) that we steered with a *graphical user interface* (GUI) created with the MATLAB GUI development environment. The GUI-controlled CNC device helped in creating a standardized and stable research and development model for the measurements. Thus, the depth and duration of the electrosurgical cuts could be accurately controlled. Each cut was approximately 4 mm deep and 5 mm long, but due to the heterogeneity of the pieces of tissue, some slight variation in height was unavoidable.

To keep the height of the cuts from varying due to the position of the knife, the electrosurgical instrument was fixed to the frame of the CNC device with a polylactic acid (PLA) holder, which in turn was connected to a medical grade surgical evacuator (SURTRON® EVAC, LED SpA, Italy) by TYGON® R-3603 Laboratory Tubing (6.4×9.6 mm, Saint-Gobain, France). We used a power level of 5 for the surgical evacuator, which corresponded to an airflow of approximately 12 l/min according to measurements we performed with Gilian Gilibrator-2 NIOSH Primary Standard Air Flow Calibrator (Sensidyne, Schauenburg International GmbH, Germany). All subsequent flow rates were also measured with the Gilibrator.

Part of the airflow that went towards the surgical evacuator was guided to the particle filtration unit by a two-fold dilution system that we constructed with M/58112/09 vacuum pump ejectors (Norgen Finland Oy, Finland). We placed the ejectors to the system so that they created a negative pressure which split the sample flow before it entered the surgical evacuator. The side flow entered the filtration unit with a flow rate of 3 l/min.

The filtration unit was a newly-patented (patent pending) corona discharge filter. The corona filter was especially applicable in this research due to its ability to effectively filter out the harmful nanoscale and microscale particles in the surgical smoke (viruses, bacteria, and soot) without causing changes to the measurement dynamics of the system through pressure differences, which would be the case for example with glass fiber filters[6]. The filtration unit and the two-fold dilution system were connected to each other with Polytetrafluoroethylene (PTFE) tubing.

Even when the large particle contaminants were removed with the filtration unit, the sample concentration of the surgical smoke was often too high for the DMS sensor. Thus, we adjusted the dilution system so that the initial sample smoke was diluted with purified dry air at a ratio of approximately 1:800 before entering the ENVI-AMC® DMS device.

In the DMS device, the sample molecules first react with the so-called reactant ions created by an Americium-241 (^{241}Am) isotope and then enter a drift chamber as sample ions. In the drift chamber, the sample ions are subjected to a radio-frequency asymmetric electric field and a superimposed direct current (DC) voltage electric field[7]. Depending on the values of both the voltage amplitude of the asymmetric waveform (V_{RF}) and the voltage of the DC compensation field (V_C), sample ions with certain mobility characteristics will reach a detector plate, which creates a pA-range electric current signal upon impact. The commonly used output response of the impact spectrum, a *dispersion plot*, presents the current signals with different values for V_{RF} (y-axis) and V_C (x-axis) as a color map. In a way, the dispersion plot can be considered

as the ‘smell fingerprint’ of the measured sample. In this study, we produced the dispersion plots by increasing the value for V_C from -0.8 V to 9.0 V with 40 equal increments and by increasing the amplitude of V_{RF} from 440 V to 770 V with four equal increments. This means that the resolution for the dispersion plots was 160 (40×4) pixels. The distance between the electrodes that form the electric field in the ENVI-AMC® is 0.25 mm, so the V_{RF} values correspond to electric field strengths of 1.76 MV/m to 3.08 MV/m. Figure 3 shows example dispersion plots for liver, lung, and subcutaneous fat.

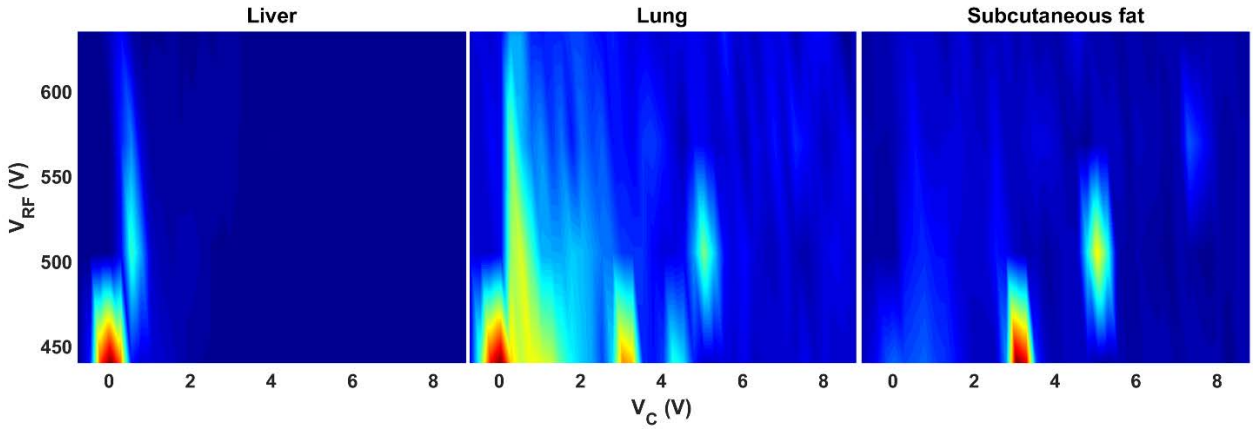

Figure 3. Example dispersion plots for liver, lung, and subcutaneous fat.

With the chosen field strengths and increments, the DMS measurement for both positive and negative ions took a total of 12 seconds per cut, after which the device cleaned itself with the dilution air for three minutes before the next measurement. This prevented any carry-over from the previous sample. A schematic representation of the measurement system and an example of an output dispersion plot from skeletal muscle tissue can be seen in Figure 4.

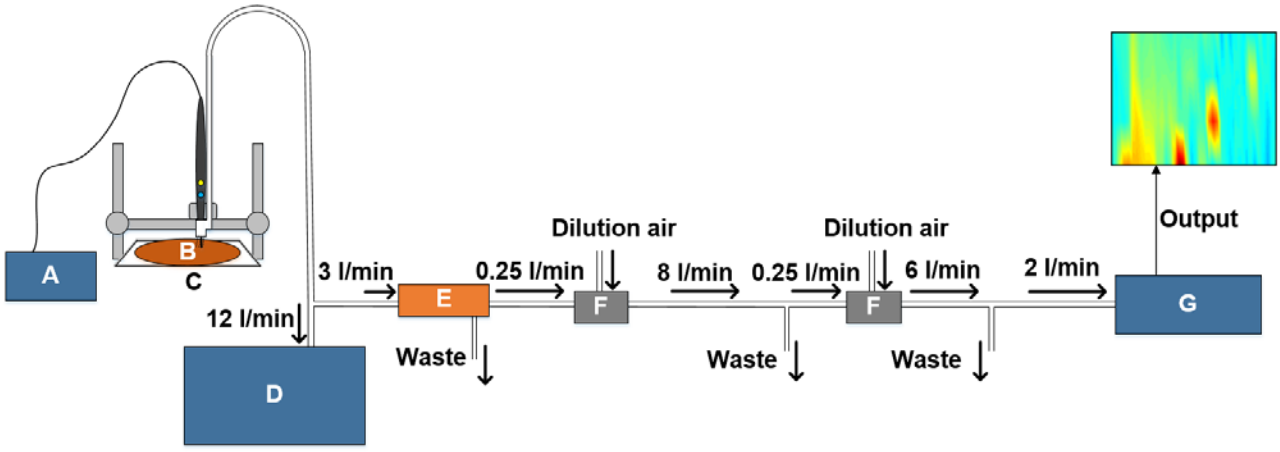

Figure 4. The measurement system. A) The Itkacut 350 MB electrosurgical unit. B) Tissue sample on the XYZ-stage of the C) CNC device. D) SURTRON® EVAC surgical evacuator. E) The filtration device. F) The dilution system. G) ENVI-AMC® differential ion mobility spectrometer.

Classification models

After each measurement set, we classified the different tissue types based on their DMS response with cross-validated *linear discriminant analysis* (LDA) models created in MATLAB (The MathWorks Inc., U.S.A). LDA is a common way to classify multi-dimensional data and it is based on reducing the dimensionality of the data by feature projection[14]. For the results in phases I and III, we cross-validated the LDA model with leave-one-out cross validation (LOOCV). For the phase II results, due to the high number of samples (600), we validated the classification model for the ten tissue types with 10-fold cross-validation. The LOOCV method is not recommended for large datasets, since the resulting training set would be almost identical with the full data set[8]. An additional validation model using 70 % of the data as training data and the remaining 30 % as test data was also done for the phase II results. This type of a *hold-out* method with 70-30 ratio for validation is a simple way to mitigate the overfitting bias in classification models, and has been commonly used in clinical studies[12].

5. Results

The results from the three measurement phases were the following:

Phase I: The five tissues were discriminated from each other and from the empty samples with a classification accuracy of 93%. One renal cortex sample was misclassified as liver and three liver samples were classified as renal cortex. All the other samples were correctly classified. The confusion matrix is presented in Table 1.

Phase II: The ten tissues were discriminated from each other with a classification accuracy of 95% by the 10-fold cross-validation model (with LOOCV, the classification accuracy was 97%). Tongue, renal cortex and skeletal muscle were most commonly misclassified. The confusion matrix is presented in Table 2. In addition to the 10-fold cross-validated results shown in Table 2, we used the phase II dataset to conduct additional validation by using 70% of the dataset to produce a classification model to discriminate the remaining 30%. The model achieved a classification accuracy of 93%. The confusion matrix for this additional model is presented in Table 3.

Phase III: The classification accuracy for the 40 measurements with four tissue types was 95%. One renal cortex sample was classified as skeletal muscle and one skeletal muscle sample was classified as liver. The confusion matrix for phase III results can be found in Table 4.

Table 1. The confusion matrix for the LDA+LOOCV classification model in phase I.[*]

Tissue	SM	SF	RC	Li	Lu	E
Skeletal muscle (SM)	10	0	0	0	0	0
Subcutaneous fat (SF)	0	10	0	0	0	0
Renal cortex (RC)	0	0	9	1	0	0
Liver (Li)	0	0	3	7	0	0
Lung (Lu)	0	0	0	0	10	0
Empty (E)	0	0	0	0	0	10

[*] LDA+LOOCV refers to leave-one-out cross-validated linear discriminant analysis. The true class of the samples is presented by the rows and the predicted class by the columns. All subsequent Tables are presented similarly.

Table 2. The confusion matrix for the 10-fold cross-validated LDA classification model in phase II.

Tissue	GM	WM	Li	SM	SF	Lu	RC	S	T	CM
Gray matter (GM)	60	0	0	0	0	0	0	0	0	0
White matter (WM)	1	59	0	0	0	0	0	0	0	0
Liver (Li)	1	0	59	0	0	0	0	0	0	0
Skeletal muscle (SM)	0	0	0	56	1	1	2	0	0	0
Subcutaneous fat (SF)	0	0	0	0	60	0	0	0	0	0
Lung (Lu)	0	0	0	0	0	55	2	0	3	0
Renal cortex (RC)	0	0	0	2	0	3	52	0	2	1
Skin (S)	0	0	0	0	0	0	1	58	1	0
Tongue (T)	0	0	0	0	0	0	6	1	52	1
Cardiac muscle (CM)	0	0	0	0	0	0	0	0	0	60

Table 3. The confusion matrix for 30% of phase II samples with the LDA classification model trained with 70 % of phase II data.

Tissue	GM	WM	Li	SM	SF	Lu	RC	S	T	CM
Gray matter (GM)	18	0	0	0	0	0	0	0	0	0
White matter (WM)	0	18	0	0	0	0	0	0	0	0
Liver (Li)	1	0	16	0	0	1	0	0	0	0
Skeletal muscle (SM)	0	0	0	16	2	0	0	0	0	0
Subcutaneous fat (SF)	0	0	0	0	18	0	0	0	0	0
Lung (Lu)	0	0	0	0	0	16	1	0	1	0
Renal cortex (RC)	0	0	0	0	0	0	16	0	2	0
Skin (S)	0	0	0	0	0	0	0	18	0	0
Tongue (T)	0	0	0	0	0	3	1	0	14	0
Cardiac muscle (CM)	0	0	0	0	0	0	0	0	0	18

Table 4. The confusion matrix for the LDA+LOOCV classification model in phase III.

Tissue	RC	SF	SM	Li
Renal cortex (RC)	9	0	1	0
Subcutaneous fat (SF)	0	10	0	0
Skeletal muscle (SM)	0	0	9	1
Liver (Li)	0	0	0	10

6. Discussion

Findings and Impact

Our results demonstrate that differential ion mobility analysis of surgical smoke can be used to differentiate healthy porcine tissues with high levels of accuracy. This finding opens up the possibility of developing an inexpensive surgical method that could be used for the near real-time assessment of tissues during electrosurgery, particularly cancer surgery. However, even though porcine tissues are a good analog for human tissues[15], in order to evaluate the clinical relevance of the technology, the findings need to be confirmed with healthy and diseased human tissues. In addition, the measurement system needs to be developed further and key ion spectrum features studied, before the method could be used in real-time analysis.

Limitations

The key limitations of our study are 1) shortcomings in the tissue specimens that limit the generalizability of the results, 2) variation in sampling and external conditions that may cause negative or positive bias to the results, 3) carry-over and the limited resolution of the dispersion plots that prevent real-time use in the current state of development.

The anatomical and mechanical variation of the tissues is also a probable cause for misclassifications. The mechanical heterogeneity of the samples with varying thickness resulted in slight variations in the cut, which changed the smoke concentration and thus, the dispersion plot. Anatomical heterogeneity is demonstrated in Figure 2 where a streak of fat is visible between muscle fibers and part of the cuts have partially hit this streak instead of pure muscle. The effect of tissue heterogeneity will be diminished as the database for the ion spectra of the tissues grows. When the properties of the ion spectra are mapped in future studies, the classification can be made by using the constant key features, which allows for more variation in the rest of the ion spectrum.

Furthermore, depending on the tissue, dispersion plots from frozen samples may differ slightly from fresh tissues. In our separate, preliminary experiments with porcine muscle tissue, there was no notable difference between the dispersion plots of fresh and frozen tissues. To generalize the results to all fresh tissues, the effect of preservation on the samples and dispersion plots needs to be explored.

Even though we standardized the electrosurgical cut, the heterogeneity of the samples led to variation in smoke concentration. This may have led to the differentiation of some tissues by the concentration of smoke rather than tissue-specific characteristics in the dispersion plots. In contrast to quantitative MS, the dispersion plot of the DMS is qualitative in nature and does not explicitly identify the detected ions or ion clusters. However, during cancer surgery, the qualitative classification of the tissue into either healthy or cancerous is sufficient for the surgeon. In the future, the concentration of smoke should be controlled to reduce bias from sampling.

The properties of the electrosurgical device may also have an effect. The device that was used in this study does not feature impedance compensation. This resulted in smoke intensity variation between the cuts, which was countered by using an

exceptionally high cutting power that might also affect the composition of the smoke, and thus the DMS response. To generalize the results to correspond with clinical use, the effect of the cutting power and impedance compensation in relation to the DMS response need to be studied further.

Additional research is also needed to find the optimal resolution for the dispersion plot. Even though the classification results were good, the DMS sweep resolution of 160 pixels is probably too low to accurately convey all the characteristic dispersion plot features of the different tissue types. The low resolution of the sweeps is a direct result of our current sampling method. In our measurements, surgical smoke was only produced during the 5 seconds of cutting, so a compromise in the resolution was needed for the DMS to match the sampling time. Low resolution is, however, only a problem in the research and development phase of the system, since the dispersion plots of the tissues are still unknown. In the future, effort should be made to increase the resolution. Higher resolution would enable researchers to more accurately study the characteristic features of the dispersion plots that are responsible for differentiating between tissues. After these features have been mapped, the DMS sweep can be concentrated on the key areas, and the measurement time will decrease to a point where it can be performed in 1–3 seconds.

Another issue that needs to be solved is carry-over. In this study, the carry-over was mitigated by a three-minute cleaning time between each cut, but a surgeon trying to distinguish tissue in the operating theatre needs a near-real-time response. This means that in order for the system to be clinically applicable, the carry-over needs to be controlled by other means.

In addition, the experimental set-up in phase II may have been subject to positive bias from the daily variations in the measurement conditions as the measurements had to be spread over several days. The absolute humidity and ambient temperature were monitored and no large shifts (>2 °C for temperature or >0.6 g/m^3 for humidity) were observed between the measurement days, but slight variations did occur. This possible variation only occurred in phase II, since the other phases were conducted in a single run of measurements during the same day.

The validation model for the phase II results (Table 3) also has potential for bias, since the measurements come from the same animal (except the brain tissues) and are spatially from a limited area. More studies are needed to conclusively prove that these results can be generalized to tissues from different pigs.

Analysis of the Results

In previous studies, porcine and other animal tissues have been identified based on surgical smoke, but the methods used have relied on complicated, expensive and bulky MS technology[5,16]. The specific molecular features that allow REIMS to differentiate porcine tissue have not been published. However, in a recent publication on the potential of using REIMS in food fraud cases[3], the method achieved 100% accuracy in determining the species that the tissue originated from. In addition, REIMS has also been used to differentiate cancerous and healthy tissue from the same organ, with above 95% sensitivity and specificity[4]. Therefore, we can assume that its performance in porcine tissue type identification will be as good as that, if not better. The classification results gained in this study are comparable and promising, when taking into account that the measurement system can still be considered an early phase prototype.

With the prototype system, the DMS responses for each tissue were different enough to enable high classification accuracy even at the low resolution of 160 pixels. This is partly explained by the different electrical properties of the tissues that lead to changes in the concentration of the smoke[17]. This phenomenon is in line with the water content of tissues[23]. However, many of the tissues (lung, liver, muscle, tongue) have similar water content, thus other factors are likely to contribute to the discrimination. REIMS studies have shown that the organic matter in the smoke from biological tissues primarily consists of various lipids (e.g. fatty acids and phospholipids) and the products of their thermal degradation[5]. These lipids are particularly common in the cell wall structures, which differ between tissue types. Even the tissues that are similar on an anatomic level such as muscle tissues (myocytes in tongue, skeletal muscle, and cardiac muscle) or neural tissues (neural cells in white matter and gray matter) exhibit different lipid profiles, which can be detected in the composition of the smoke[11].

In addition to the differences in smoke composition, and lipids, other molecules explain some of the characteristics in the dispersion plots as well as some of the misclassifications. The DMS responses for liver and renal cortex seemed to be mostly concentrated in the region of heavy volatile organic compounds (VOCs), reflected in the dispersion plots as the dominance of the ion peak at $V_C = 0$ (Figure 3). Especially in phase I, the liver and renal cortex were partly classified as each other. The misclassifications and abundant heavy VOCs can be due to metabolic waste compounds, such as bilirubin in liver and various bodily toxins in kidneys.

Aside from the liver and renal cortex in phase I, the most common misclassifications (especially in phase II) were between the tongue and renal cortex. According to chemical analysis of normal human tissues, the general composition of kidney and muscle tissue is very similar[23]. There is no comprehensive data on the molecular composition of porcine tissues. An extensive database on mouse tissue compositions did not yield findings relevant to our work[19]. The lack of relevant data on human and animal tissues with molecular profiling methods, such as MS or nuclear magnetic resonance, highlights the need for more of such studies on normal tissues.

Even though the tissue biology can partly explain the classification results, the limitations of the system and the variability of the tissue material also have to be considered. Some of the misclassifications are due to the variation within the class responses. Physical or anatomical heterogeneity and blood vessels most probably caused some tissue classes to exhibit higher variations in their ion spectrums. This, combined with the relatively low resolution, made the prediction for the classification model much more difficult.

Conclusions

We have shown that the DMS-driven differentiation of porcine tissues based on surgical smoke is possible. This study is a first step towards a novel method for surgical smoke analysis, which can foreseeably be used to discriminate between malignant and benign human tissue in the future. However, when interpreting the results, the limitations of the study need to be acknowledged. The system itself requires improvements, and additional testing using various tissue materials is needed. In addition, the method’s capacity to differentiate between diseased and healthy human tissue still has to be proven.

Almost all types of electrosurgically operated cancers can provide material for new research advancements. Further reliable and satisfactory results can eventually lead

to the commercialization of the method. The low cost and simplicity of the DMS could make the method accessible for global clinical use.

7. Acknowledgements

This study was supported by grants from the following foundations: Finnish Cultural Foundation, South Savo Regional fund, Finnish Foundation for Technology Promotion (TES), Tampereen Tuberkuloosisäätiö (Tampere Tuberculosis Foundation), Emil Aaltonen foundation and Pirkanmaan sairaanhoitopiiri (PSHP) grants 9s045, 151B03, 9T044, 9U042 and 150618.

The study material used in the research was slaughterhouse offal. Ethical approval from the Ethics Committee of the Tampere Region was not needed for conducting this research, as confirmed from the committee itself.

Authors Markus Karjalainen, Antti Roine, Niku Oksala, and Jukka Lekkala are shareholders of Olfactomics Ltd (www.olfactomics.fi), a company developing applications for eNose technology.

The authors would like to thank D.Sc. Ville Rantanen, D.Sc. Pekka Kumpulainen, and Assistant Professor Antti Vehkaoja for their comments and contributions to the final manuscript.

This is a post-peer-review, pre-copyedit version of an article published in [insert journal title]. The final authenticated version is available online at: http://dx.doi.org/10.1007/s10439-018-2035-5

8. References

1. Allweis, T. M., Z. Kaufman, S. Lelcuk, I. Pappo, T. Karni, S. Schneebaum, R. Spector, A. Schindel, D. Hershko, M. Zilberman, J. Sayfan, Y. Berlin, A. Hadary, O. Olsha, H. Paran, M. Gutman, and M. Carmon. A prospective, randomized, controlled, multicenter study of a real-time, intraoperative probe for positive margin detection in breast-conserving surgery. *Am. J. Surg.* 196:483–489, 2008.

2. Baggish, M. S., R. F. Valle, and H. Guedj. Hysteroscopy: Visual perspectives of uterine anatomy, physiology and pathology. Lippincott Williams & Wilkins, 2007, 125 pp.

3. Balog, J., D. Perenyi, C. Guallar-Hoyas, A. Egri, S. D. Pringle, S. Stead, O. P. Chevallier, C. T. Elliott, and Z. Takats. Identification of the Species of Origin for Meat Products by Rapid Evaporative Ionization Mass Spectrometry. *J. Agric. Food Chem.* 64:4793–4800, 2016.

4. Balog, J., L. Sasi-Szabó, J. Kinross, M. R. Lewis, L. J. Muirhead, K. Veselkov, R. Mirnezami, B. Dezso, L. Damjanovich, A. Darzi, J. K. Nicholson, and Z. Takáts. Intraoperative tissue identification using rapid evaporative ionization mass spectrometry. *Sci. Transl. Med.* 5:, 2013.

5. Balog, J., T. Szaniszló, K.-C. Schaefer, J. Denes, A. Lopata, L. Godorhazy, D. Szalay, L. Balogh, L. Sasi-Szabó, M. Toth, and Z. Takáts. Identification of biological tissues by rapid evaporative ionization mass spectrometry. *Anal. Chem.* 82:7343–7350, 2010.

6. Bardin-Monnier, N., and D. Thomas. 3 - Initial Pressure Drop for Fibrous Media BT - Aerosol Filtration. Elsevier, 2017, pp. 49–78.

7. Eiceman, G. A., Z. Karpas, and H. H. Hill Jr. Ion mobility spectrometry. CRC press, 2013, 1-293 pp.

8. Izenman, A. J. Recursive Partitioning and Tree-Based Methods BT - Modern Multivariate Statistical Techniques: Regression, Classification, and Manifold Learning. edited by A. J. Izenman. New York, NY: Springer New York, 2008, pp. 281–314.doi:10.1007/978-0-387-78189-1_9

9. Kupstas, A., W. Ibrar, R. D. Hayward, D. Ockner, C. Wesen, and J. Falk. A novel modality for intraoperative margin assessment and its impact on re-excision rates in breast conserving surgery. *Am. J. Surg.* , 2017.doi:https://doi.org/10.1016/j.amjsurg.2017.11.023

10. Munro, M. G. Fundamentals of Electrosurgery Part I: Principles of Radiofrequency Energy for Surgery BT - The SAGES Manual on the Fundamental Use of Surgical Energy (FUSE). edited by L. Feldman, P. Fuchshuber, and D. B. Jones. New York, NY: Springer New York, 2012, pp. 15–59.

11. Nikolaidis, M. G., A. Petridou, and V. Mougios. Comparison of the phospholipid

and triacylglycerol fatty acid profile of rat serum, skeletal muscle and heart. *Physiol. Res.* 55:259, 2006.

12. Pang, H., and S.-H. Jung. Sample Size Considerations of Prediction-Validation Methods in High-Dimensional Data for Survival Outcomes. *Genet. Epidemiol.* 37:276–282, 2013.

13. Pataky, R. E., and C. R. Baliski. Reoperation costs in attempted breast-conserving surgery: A decision analysis. *Curr. Oncol.* 23:314–321, 2016.

14. Quadrianto, N., and W. L. Buntine. Linear Discriminant. In: Encyclopedia of Machine Learning, edited by C. Sammut, and G. I. Webb. Boston, MA: Springer US, 2010, pp. 601–603.doi:10.1007/978-0-387-30164-8_475

15. Roth, J. A., and C. K. Tuggle. Livestock models in translational medicine. *ILAR J.* 56:1–6, 2015.

16. Schäfer, K.-C., J. Dénes, K. Albrecht, T. Szaniszló, J. Balog, R. Skoumal, M. Katona, M. Tóth, L. Balogh, and Z. Takáts. In Vivo, In Situ Tissue Analysis Using Rapid Evaporative Ionization Mass Spectrometry. *Angew. Chemie Int. Ed.* 48:8240–8242, 2009.

17. Sharp, J., K. Bouazza-Marouf, D. Noronha, and A. Gaur. Tissue type determination by impedance measurement: A bipolar and monopolar comparison. *Saudi J. Anaesth.* 11:15–20, 2017.

18. St John, E. R., J. Balog, J. S. McKenzie, M. Rossi, A. Covington, L. Muirhead, Z. Bodai, F. Rosini, A. V. M. Speller, S. Shousha, R. Ramakrishnan, A. Darzi, Z. Takats, and D. R. Leff. Rapid evaporative ionisation mass spectrometry of electrosurgical vapours for the identification of breast pathology: Towards an intelligent knife for breast cancer surgery. *Breast Cancer Res.* 19:, 2017.

19. Sugimoto, M., S. Ikeda, K. Niigata, M. Tomita, H. Sato, and T. Soga. MMMDB: mouse multiple tissue metabolome database. *Nucleic Acids Res.* 40:D809--D814, 2011.

20. Ulmer, B. C. The Hazards of Surgical Smoke. *AORN J.* 87:721–738, 2008.

21. Verplanken, K., S. Stead, R. Jandova, C. V Poucke, J. Claereboudt, J. V Bussche, S. D. Saeger, Z. Takats, J. Wauters, and L. Vanhaecke. Rapid evaporative ionization mass spectrometry for high-throughput screening in food analysis: The case of boar taint. *Talanta* 169:30–36, 2017.

22. Watson, J. T., and O. D. Sparkman. Introduction to mass spectrometry: instrumentation, applications, and strategies for data interpretation. John Wiley & Sons, 2007, 25-26 pp.

23. Woodard, H. Q., and D. R. White. The composition of body tissues. *Br. J. Radiol.* 59:1209–1218, 1986.